RESEARCH ARTICLE

Design and Characterization of Buccal Patch Containing Extracts of *Ailanthus excelsa* and *Tridax procumbens* for the Treatment of Inflammation

Yogesh B. Ubarhande*, Ashish Singh Parihar

[*]*Faculty of Pharmacy, Oriental University Indore, Jakhya, Indore, Madhya Pradesh 453555, India*

Received: 17th Dec, 2024; Revised: 24th Jan, 2025; Accepted: 16th Feb, 2025; Available Online: 25th Mar, 2025

ABSTRACT

Inflammation is a natural immune response, but chronic inflammation can lead to various diseases, including arthritis, cardiovascular disorders, and autoimmune conditions. *Ailanthus excelsa* and *Tridax procumbens* possess anti-inflammatory properties, making them valuable for medicinal use. This study develops and evaluates buccal patches incorporating their extracts for inflammation management. Extracts were characterized using UV-Vis, FTIR, and DSC analyses, confirming compatibility with excipients. Buccal Patches, formulated using HPMC, PVA, and glycerol, were optimized via Central Composite Design and evaluated for mechanical and drug release properties. UV-Vis spectroscopy identified absorption peaks at 254 nm and 240 nm, while FTIR analysis confirmed functional groups indicative of a complex organic composition. DSC analysis revealed phase transitions at 96.34°C and 339.48°C, ensuring thermal stability. FTIR and DSC studies showed no significant interactions between extracts and excipients, confirming formulation stability. Optimized patches, formulated with HPMC K100, PVA, and glycerol, exhibited tensile strength between 0.567 to 0.987 kg/cm² and drug release of 85.74% to 97.21%. Statistical analysis confirmed polymer concentration's impact on mechanical properties and drug release. In conclusion, the study successfully developed extract-loaded buccal patches with optimal mechanical strength and controlled drug release, highlighting their potential as an efficient drug delivery system. Future research should focus on *in vivo* evaluation, long-term stability, and patient adherence for clinical applications.

Keywords: Inflammation, *Ailanthus excels, Tridax procumbens*, Buccal Patch, UV-Vis spectroscopy

How to cite this article: Yogesh B. Ubarhande, Ashish Singh Parihar. Design and Characterizations of Buccal Patch Containing Extracts of *Ailanthus excelsa* and *Tridax procumbens* for the Treatment of Inflammation. International Journal of Drug Delivery Technology. 2025;15(1):205-15. doi: 10.25258/ijddt.15.1.29

Source of support: Nil

Conflict of interest: None

INTRODUCTION

Inflammation is a fundamental biological response to injury or infection, characterized by erythema, edema, hyperthermia, and nociception. Although it functions as a protective mechanism, persistent inflammation can lead to several illnesses, including as arthritis, cardiovascular issues, and autoimmune ailments [1]. Conventional therapies for inflammation, including nonsteroidal anti-inflammatory medications (NSAIDs) and corticosteroids, frequently have adverse effects that restrict their prolonged application. Consequently, the pursuit of alternative medicines with natural ingredients has garnered considerable interest in recent years [2]. Herbal therapy has been integral to traditional healthcare systems for generations. *Ailanthus excelsa* and *Tridax procumbens* are two native plants recognized for their established therapeutic capabilities, including anti-inflammatory, antibacterial, and wound-healing actions. *Ailanthus excelsa*, or Tree of Heaven, is abundant in flavonoids, alkaloids, and phenolic chemicals that enhance its pharmacological properties. *Tridax procumbens*, often known as coat buttons, has been thoroughly investigated for its wound-healing, antioxidant, and anti-inflammatory properties. The bioactive components in these plants provide them interesting candidates for the development of innovative anti-inflammatory compositions [3–7]. The buccal route of medication delivery presents several benefits compared to traditional oral and topical techniques. Buccal patches facilitate prolonged medication release, enhanced bioavailability, and increased patient adherence by circumventing first-pass metabolism. These patches attach to the mucosal surface, facilitating direct medication absorption into systemic circulation, so serving as an effective and non-invasive option for controlling inflammatory illnesses [8–10]. The integration of *Ailanthus excelsa* and *Tridax procumbens* extracts into buccal patches offers an innovative approach for localized and systemic anti-inflammatory effects. The development of an efficient buccal patch necessitates meticulous attention to formulation and characterisation criteria. The choice of an appropriate polymeric foundation guarantees optimal adhesion, drug release kinetics, and mechanical integrity. The physicochemical parameters, including thickness, tensile strength, swelling behavior, and moisture content, are crucial in assessing the efficacy and stability of the patch [9]. Furthermore, *in vitro* and *ex vivo* investigations of drug release, penetration, and anti-inflammatory efficacy are crucial for determining its therapeutic potential. This

**Author for Correspondence: yogeshuv@gmail.com*

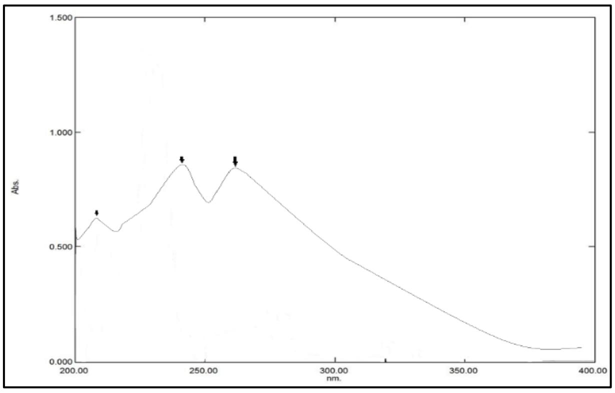

Figure 1: UV Spectrum of Both Extracts

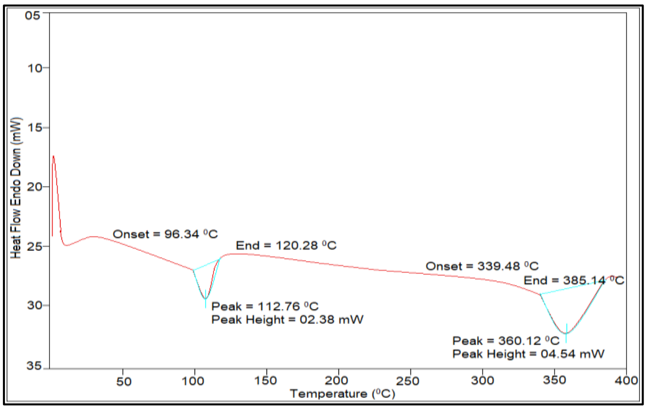

Figure 2: It shows DSC Spectrum of Both Extracts

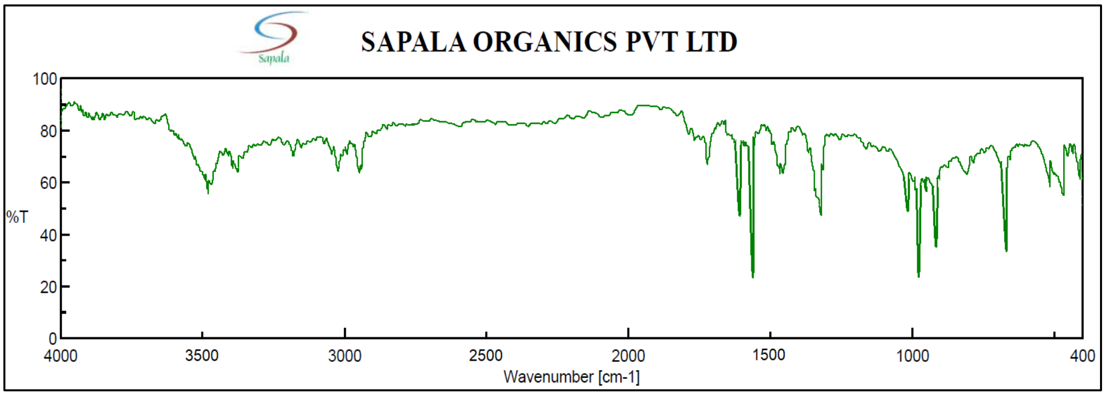

Figure 3: It shows FTIR Spectrum of Both Extracts

Table 1. Variables and levels

Variable	(-1) Low level	(+1) High level
Independent		
A= HPMC	10mg	20mg
B= PVA	5mg	10mg
C= Glycerol	2ml	4ml
Dependent		
Y1= Tensile strength		
Y2 = % DR at 12th day		

research intends to formulate and analyze buccal patches including extracts of *Ailanthus excelsa* and *Tridax procumbens* for the management of inflammation. The formulation will be refined based on physicochemical evaluations, drug release analyses, and anti-inflammatory assessments. This research aims to utilize the bioactive properties of plant extracts in a buccal delivery system to offer a natural and effective option for inflammation management, while reducing the bad effects linked to traditional medications [11,12]. The results of this study may enhance the expanding domain of herbal pharmaceutical formulations and foster the advancement of safer, more sustainable therapies for inflammatory conditions.

MATERIAL AND METHODS

Procurement, Identification and Authentication

Extracts were commercially available cosmetic grade ingredients and were donated by Sunpure Extract Pvt. Ltd. India. The plant was recognized and validated from

Table 2. Formulation batches of Patch.

Batches	Factor		
	A: HPMC (mg)	B: PVA (mg)	C: Glycerol (ml)
F1	10	5	4
F2	20	10	2
F3	15	7.5	3
F4	20	5	2
F5	6.59104	7.5	3
F6	20	10	4
F7	15	7.5	1.31821
F8	15	7.5	3
F9	15	11.7045	3
F10	15	7.5	3
F11	15	7.5	3
F12	10	10	4
F13	15	7.5	3
F14	20	5	4
F15	15	7.5	4.68179
F16	10	10	2
F17	10	5	2
F18	23.409	7.5	3
F19	15	3.29552	3
F20	15	7.5	3

Botanical Survey of India, Western Regional Center, Pune, Maharashtra, India.

Physical Characterization of Extracts

UV Determinations, FTIR, and DSC Analysis
The plant extracts were analyzed using UV-Visible spectroscopy. The sample was diluted to a ratio of 1:10 using the identical solvent. The extract was analyzed within the wavelength range of 200-800 nm using a Perkin Elmer Spectrophotometer, and the typical peaks were identified. FTIR analysis was conducted using an FTIR spectrometer (Version 7.03 Shimadzu, Japan) with a KBr disc [13]. A thermogram for *Ailanthus excelsa* and *Tridax procumbens* extract was acquired utilizing differential scanning

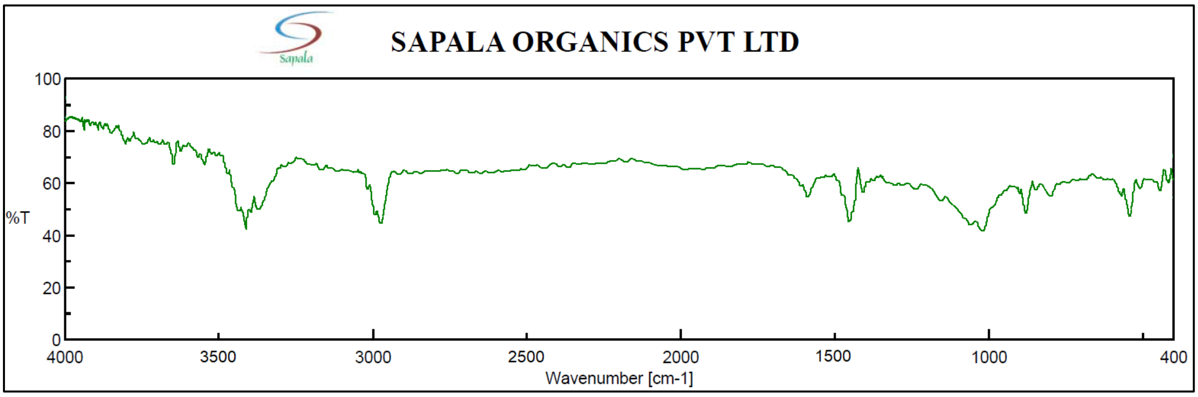

Figure 4. FTIR spectra of HPMC K100

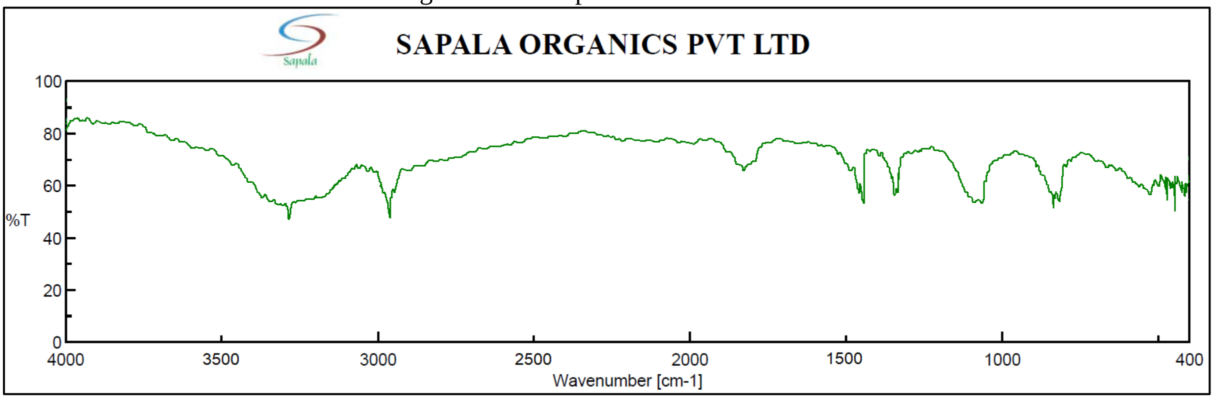

Figure 5. FTIR spectra of PVA

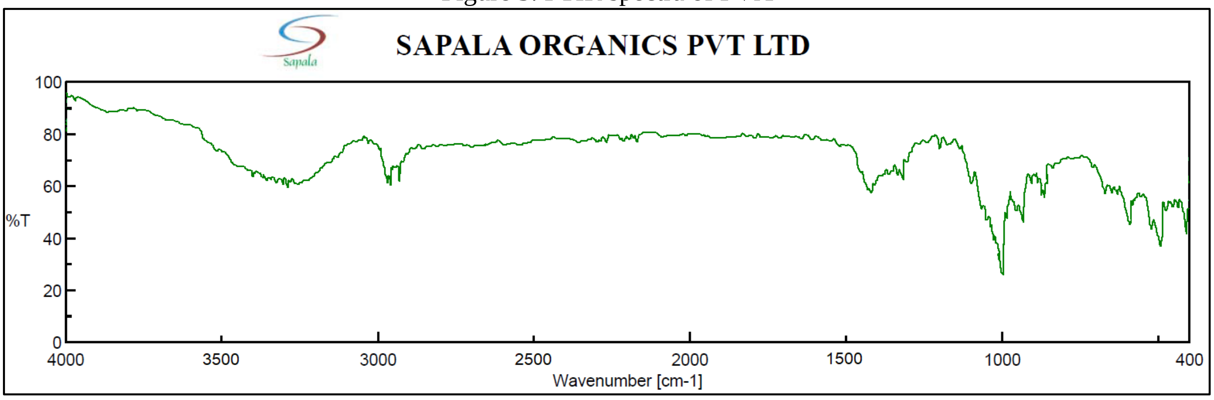

Figure 6. FTIR spectra of Glycerol

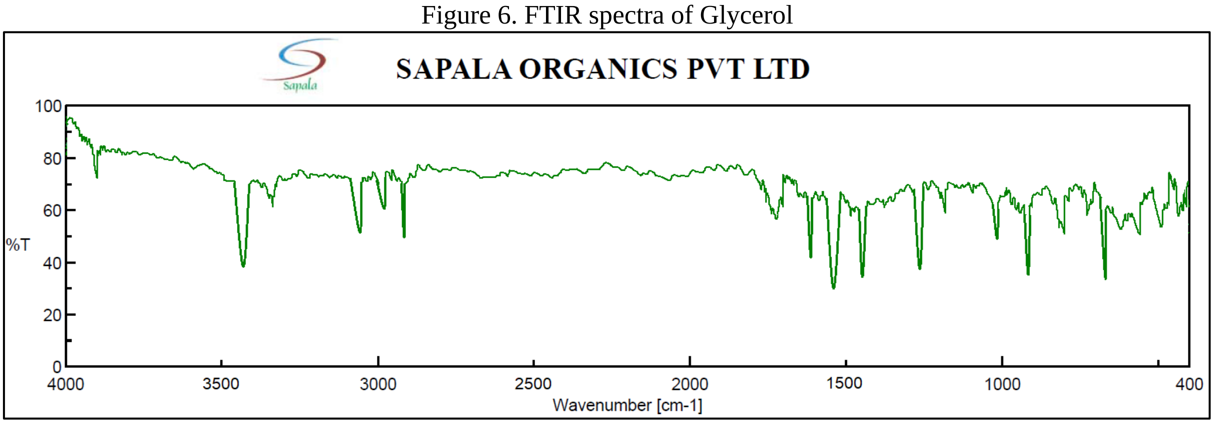

Figure 7. FTIR spectra of extracts with Physical Mixture

calorimetry (DSC) with a Mettler DSC 1-star system from Mettler-Toledo, Switzerland.

Drug-Excipients Compatibility Study

FTIR and DSC Analysis

FTIR and DSC analysis of *Ailanthus excels*, *Tridax procumbens* and different polymers along with physical mixture were done to understand the physical and chemical compatibilities.

Formulation Designs

Preparation of Extracts-Loaded HPMC Patch using CCD full factorial designs

Statistical Design of experiments (DOE)

The design of CCD was employed in the creation and optimization of extracts-loaded buccal patches. The concentrations of HPMC (A, mg), PVA (B, mg), and Glycerol (C, ml) were treated as independent factors, manipulated at two levels (-1 and +1), while tensile strength (Y1) and in vitro drug release (%CDR) (Y2) were regarded as dependent variables [14,15]. The specifics of the factors and the three levels are detailed in Table 1.

Development of Extracts-loaded HPMC Patch

Solvent casting was employed to produce HPMC (K100) patches with a loading of 2 mg of each pure extract. To enhance the tensile strength of the patches, PVA was used,

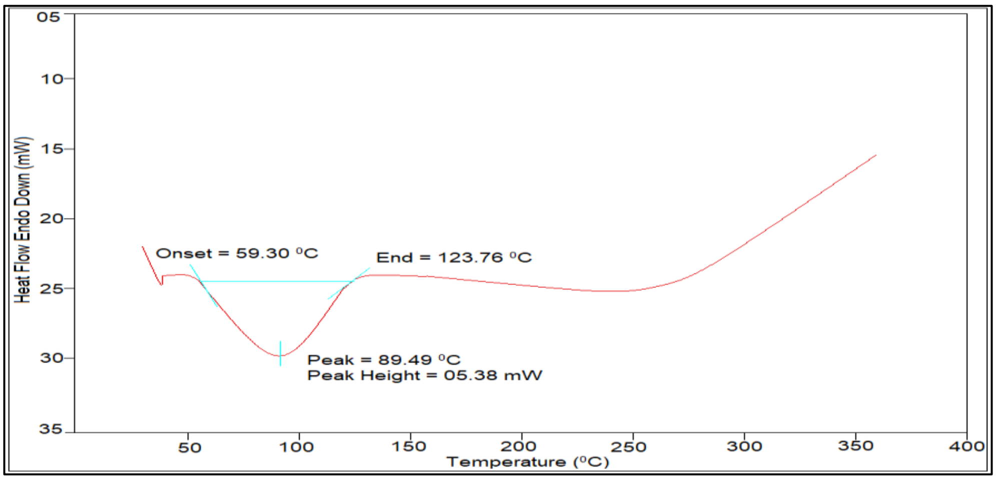

Figure 8. DSC spectra of HPMC K100

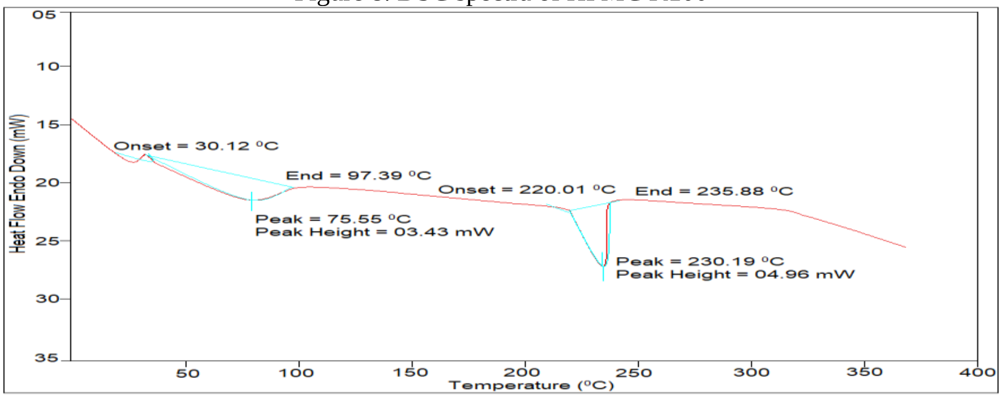

Figure 9. DSC spectra of PVA

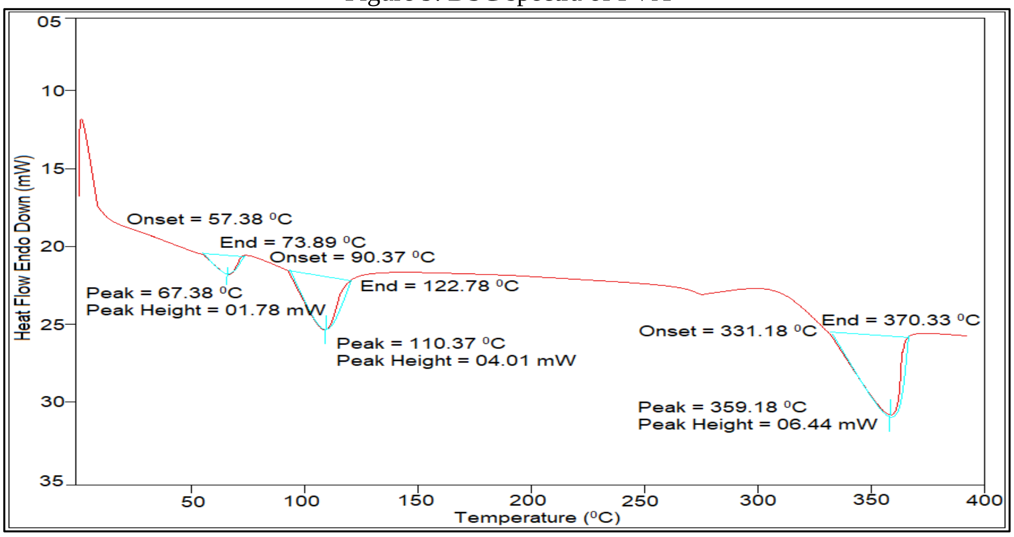

Figure 10. DSC spectra of both extracts with Physical Mixture

Table 3. Extracts loaded Patches with coded form and their responses

Batch	Factor			Response	
	A: HPMC (mg)	B: PVA (mg)	C: Glycerol (ml)	Y1 (kg/cm^2)	Y2 (%)
F1	10	5	4	0.745	92.24
F2	20	10	2	0.567	97.21
F3	15	7.5	3	0.575	89.43
F4	20	5	2	0.767	92.11
F5	6.59104	7.5	3	0.689	91.61
F6	20	10	4	0.625	89.16
F7	15	7.5	1.31821	0.782	92.78
F8	15	7.5	3	0.585	89.61
F9	15	11.7045	3	0.679	90.67
F10	15	7.5	3	0.669	89.21
F11	15	7.5	3	0.579	95.68
F12	10	10	4	0.711	90.81
F13	15	7.5	3	0.577	90.67
F14	20	5	4	0.745	89.87
F15	15	7.5	4.68179	0.791	91.68
F16	10	10	2	0.721	94.25
F17	10	5	2	0.987	85.74
F18	23.409	7.5	3	0.573	90.91
F19	15	3.29552	3	0.702	90.88
F20	15	7.5	3	0.581	90.78

Table 4. ANOVA of Y1

Source	Sum of Squares	df	Mean Square	F-value	p-value	
Model	0.1814	9	0.0202	6.16	0.0044	significant
A-HPMC	0.0314	1	0.0314	9.60	0.0113	
B-PVA	0.0318	1	0.0318	9.70	0.0110	
C-Glycerol	0.0030	1	0.0030	0.9025	0.3645	
AB	0.0001	1	0.0001	0.0153	0.9041	
AC	0.0104	1	0.0104	3.17	0.1055	
BC	0.0122	1	0.0122	3.72	0.0827	
A^2	0.0047	1	0.0047	1.44	0.2579	
B^2	0.0221	1	0.0221	6.74	0.0267	
C^2	0.0769	1	0.0769	23.50	0.0007	
Residual	0.0327	10	0.0033			
Lack of Fit	0.0260	5	0.0052	3.85	0.0826	not significant
Pure Error	0.0067	5	0.0013			
Cor Total	0.2141	19				

while HPMC was utilized as a patch-forming and gelling agent. Twenty milliliters of distilled water were utilized to fully dissolve a measured quantity of HPMC (K100) polymer. A magnetic stirrer was employed to blend the homogeneous mixture with the PVA solution, which had been previously dissolved in hot water. Glycerol was incrementally introduced in accurately quantified volumes while the polymeric dispersion was continually agitated to achieve a uniform mixture. The weighed extracts were diluted in a minimal volume of water, incorporated into the polymer solution, and well mixed. The combination was placed in a petri dish and allowed to stand at room temperature to facilitate the evaporation of the solvent from the solution [16]. The fabricated buccal patches were removed from the petri dish and kept in desiccators until required.

Table 2 presents the details of the batches in coded format.

Evaluation of Patch

Evaluation of patch loaded both extracts were carried for following parameters.

Patch Thickness

Using screw gauges, we tested the patch's thickness in several spots and averaged the results.

Consistency of the patch's weight

Multiple sections of the patch were sampled, each with a 5x5 mm patch size. It was determined how much each patch's weight changed.

Folding strength

To test the patch's folding durability, we folded it in the same spot multiple times until it broke or folded, an acceptable test that shows the patch has excellent qualities. We ran this test across the whole patch.

Ensuring consistent drug content in patches

A 5x5 mm patch was extracted from different parts of patch and placed into a 100 ml volumetric flask, to which 100 ml of water had been added then placed aside until the patch fully dissolved. The absorbance of the mixture was

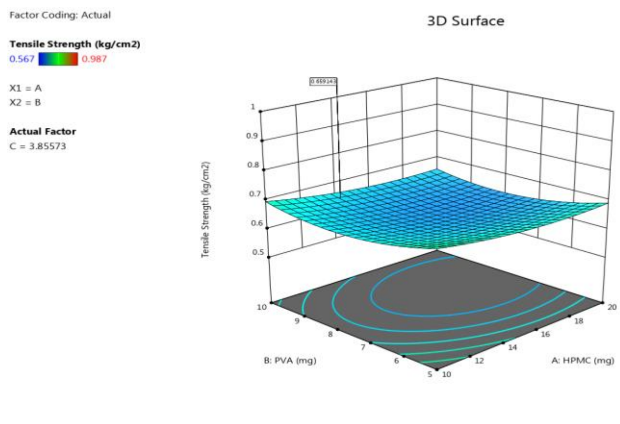

Figure 11 (A. 3D surface responses of HPMC, PVA and Glycerol on tensile strength

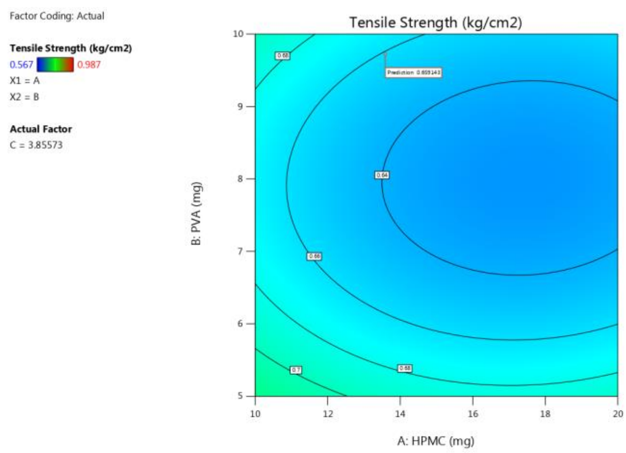

Figure 11 (B). Contour Plot of HPMC, PVA and Glycerol on tensile strength

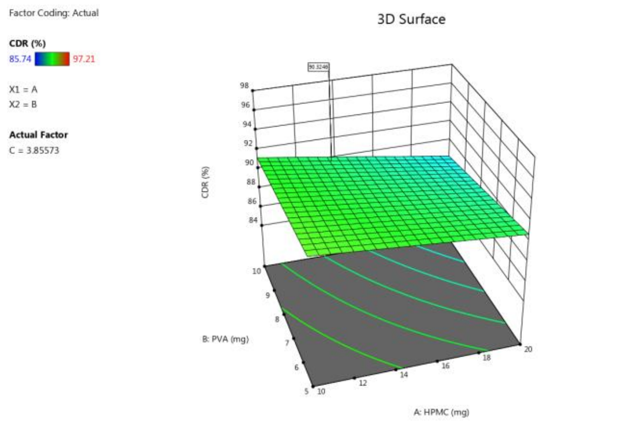

Figure 12 (A). 3D surface responses of HPMC, PVA and glycerol on %CDR

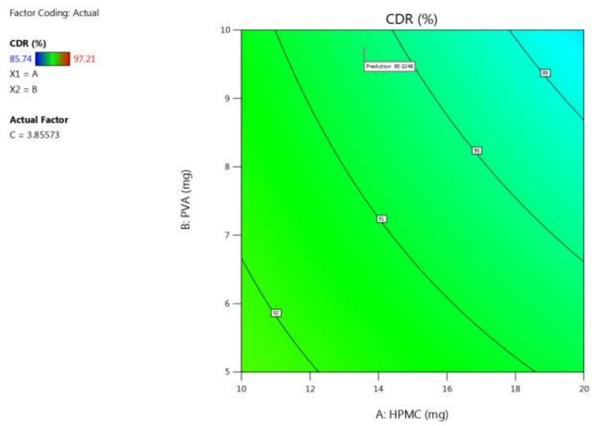

Figure 12 (B). Contour Plot of HPMC, PVA and glycerol on %CDR

determined at the corresponding wavelength.

Loss of Moisture

The samples of various concentrations were precisely weighed, placed in desiccators for three days, reweighed, and moisture loss was estimated using the formula % method.

(Initial wt. – final wt./initial wt.) ×100------ (1)

Tensile strength of the patch

Tensile strength was evaluated using a tensile strength tester (Brookfield Engineering Labs, Inc.) with a 5 g load cell. Patch of the required dimension and free from air bubbles or physical imperfections were held between two clamps. During measurement, the top clamp, at a rate of 0.5 mm/s, was pulled, and the force was measured when the patch broke. Only results from patch samples that broke between the clamps were used.

In vitro release studies

The pH of gingival fluid is within the range of 6.5-6.8; therefore, the phosphate buffer with a pH of 6.8 was used as simulated gingival fluid. Since the patch was needed to remain fixed in the pouch, a static dissolution model was employed for the dissolution studies. Known weight and patch dimensions were set to sets of six patches that were separately set into small sealed 1 ml test tubes each containing 1.0 ml phosphate buffer with a pH of 6.8. The test tubes were then placed at 37±0.5°C for 24 hours. After this period, the buffer was removed and a second 1.0 ml of fresh buffer was added. The concentration of the drug was measured using a UV/VIS spectrophotometer at Ailanthus excels (254 nm) and Tridax procumbens (240 nm).

Analyzing stability

For the stability trials, the improved formulations were kept wrapped in aluminum foil and butter paper at a temperature of 40±2°C and a relative humidity of 75%±6% for a period of two months. After the stability tests completed, the samples were checked and compared to the initial findings.

RESULT AND DISCUSSION

Physical Characterization and Identification of Extract

UV Determinations

The UV-Vis spectrophotometer concerns to the spectroscopy of photons within the UV-Vis spectrum. UV-Vis spectroscopy employs light within the visible spectrum or its adjacent wavelengths. The colors of the compounds involved directly influences absorption within the visible spectrum. Molecules experience electronic transitions within these regions of the electromagnetic spectrum [17]. In the present study UV-Vis spectral profile show the peaks of *Ailanthus excels* (254nm) and *Tridax procumbens* (240nm) in Figure 1.

Table 5. ANOVA of Y2

Source	Sum of Squares	df	Mean Square	F-value	p-value	
Model	70.53	6	11.75	3.31	0.0333	significant
A-HPMC	1.25	1	1.25	0.3525	0.5629	
B-PVA	9.05	1	9.05	2.55	0.1343	
C-Glycerol	6.04	1	6.04	1.70	0.2147	
AB	0.9045	1	0.9045	0.2549	0.6221	
AC	22.28	1	22.28	6.28	0.0263	
BC	31.01	1	31.01	8.74	0.0111	
Residual	46.13	13	3.55			
Lack of Fit	16.53	8	2.07	0.3491	0.9101	not significant
Pure Error	29.60	5	5.92			
Cor Total	116.65	19				

Table 6. Mechanical properties of HPMC K100 patch

Formulations	Thickness (mm)	Weight variation (mg)	Folding endurance	Tensile strength (kg/cm^2)
F1	0.315 ±0.04	8.38 ±0.15	272.5 ±0.12	0.745
F2	0.316 ±0.05	8.45 ±0.12	289.9 ±0.24	0.567
F3	0.312 ±0.02	7.68 ±0.04	275.9 ±0.30	0.575
F4	0.352 ±0.02	8.18 ±0.05	250.8 ±0.35	0.767
F5	0.368 ±0.07	9.05 ±0.03	236.6 ±0.37	0.689
F6	0.348 ±0.05	7.74 ± 0.12	249.0 ±0.39	0.625
F7	0.384 ±0.03	10.06 ±0.03	235.7 ±0.25	0.782
F8	0.372 ±0.01	10.26 ±0.03	240.4 ±0.44	0.585
F9	0.384 ±0.04	10.1 ±0.08	254.9 ±0.28	0.679
F10	0.298±0.07	10.02±0.09	250.1 ±0.22	0.669
F11	0.297±0.03	8.40 ±0.11	248.3 ±0.17	0.579
F12	0.300±0.05	8.59 ±0.13	262.5 ±0.27	0.711
F13	0.298±0.04	9.12 ±0.21	259.4 ±0.35	0.577
F14	0.296±0.02	9.17 ±0.05	265.8 ±0.42	0.745
F15	0.299±0.03	9.59 ±0.17	287.1 ±0.12	0.791
F16	0.288±0.04	8.38 ±0.15	314.4 ±0.17	0.721
F17	0.291±0.06	9.87 ±0.12	272.1 ±0.21	0.987
F18	0.321	9.67±0.10	267.1 ±0.11	0.573
F19	0.304	9.61 ±0.14	254.7 ±0.21	0.702
F20	0.299	9.61 ±0.27	269.4 ±0.31	0.581

FTIR Analysis

FTIR has emerged as an essential instrument for identifying and characterising compounds and chemical bonds. This technique enables the qualitative analysis of organic substances through the detection of specific frequency bands in the infrared spectrum. These bands are further influenced by the neighbouring functional groups, providing valuable information about the molecular structure [18]. The FTIR spectrum indicates the presence of carboxylic acids (O-H, 3333.89 cm^{-1}), alkanes (C-H, 2919.00, 2109.96, and 2054.48 cm^{-1}), aldehydes (C-H, 2850.71 cm^{-1}; C=O, 1604.43 and 1157.60 cm^{-1}), ketones (C=O, 1718.46 cm^{-1}), amides (C=O, 1636.89 cm^{-1}), aromatic carbons (C=C, 1448.35 cm^{-1}), amines (C-N, 1199.94, 1071.07, and 1033.33 cm^{-1}), and haloalkanes (C-F, 1376.51, 1279.28, 1242.91, and 1101.60 cm^{-1}; C-Cl, 899.90, 861.49, 740.52, and 656.88 cm^{-1}). This reflects a complex mixture of functional groups and organic compounds.

Differential Scanning Calorimetry

The Differential Scanning Calorimetry (DSC) examination of both extracts, performed at a 10°C/min scanning rate, revealed a distinct melting endothermic peak at 96.34ºC and 339.48ºC, as shown in Figure 3. This peak indicates the transition from a semi-solid to a liquid state, demonstrating the heat flow associated with this phase change. Moreover, as the temperature increases, certain components of the NP may undergo decomposition, emitting energy in the process. This breakdown is evident on the DSC curve as an endothermic peak, indicative of the heat absorbed during this particular thermal conditions [19,20].

Drug-Excipients Compatibility Study

FTIR Analysis

In Figure 2, 4-7 the FTIR spectra are depicting the both extracts and the physical mixture comprising all excipients. The FTIR spectra exhibit indicates the presence of carboxylic acids, alkanes, aldehydes, ketones, aromatic carbons, amines, and halo-alkanes respectively. Notably, all these peaks remain unchanged, showing no significant alterations in the characteristic peaks of the extracts when compared to the physical mixture [18].

Differential Scanning Calorimetry

Differential Scanning Calorimetry (DSC) has been proposed as a rapid technique to evaluate the physical and chemical interactions within a formulation. It includes comparison of the temperature profiles of pure substances

Table 7. Physicochemical properties of HPMC K100 patch

Formulations	Drug content (%)	% Moisture loss	Drug release (%)
F1	92.37 ±0.42	4.01 ±0.04	92.24
F2	93.56 ±0.44	3.2 ±0.03	97.21
F3	90.66 ±0.56	4.1 ±0.06	89.43
F4	89.00 ±0.54	2.6 ±0.03	92.11
F5	88.65 ±0.66	5.3 ±0.04	91.61
F6	91.87 ±0.36	4.04 ±0.06	89.16
F7	90.78 ±0.74	3.3 ±0.05	92.78
F8	87.96 ±0.65	4.5 ±0.02	89.61
F9	85.54 ±0.59	2.3 ±0.06	90.67
F10	95.11 ±0.45	3.9±0.11	89.21
F11	96.17 ±0.65	4.1±0.14	95.68
F12	97.24 ±0.70	3.8±0.12	90.81
F13	95.87 ±0.52	3.9±0.17	90.67
F14	96.18 ±0.64	4.0±0.10	89.87
F15	95.24 ±0.11	3.9±0.10	91.68
F16	98.50 ±0.55	2.5±0.08	94.25
F17	94.25 ±0.77	4.1±0.07	85.74
F18	97.24 ±0.55	5.2±0.26	90.91
F19	95.22 ±0.63	4.8±0.72	90.88
F20	98.11 ±0.24	4.5±0.11	90.78

Table 8. *In-vitro* release profile of optimized buccal patch

Sr. No.	Time (Hours)	F17
1	0	0
2	2	12.24±0.04
3	4	24.43±0.03
4	6	48.26±0.02
5	8	61.25±0.09
6	10	70.35±0.03
7	12	81.31±0.01
8	24	85.74±0.04

Table 9. Standard calibration curve of both extracts in pH 6.8

Sr. No	Concentration (µg/ml)	Absorbance	Absorbance
1	0	0	0
2	10	0.118±0.02	0.133±0.01
3	20	0.263±0.04	0.289±0.02
4	40	0.391±0.08	0.412±0.05
5	60	0.603±0.06	0.615±0.07
6	80	0.839±0.07	0.814±0.09
7	100	0.967±0.05	0.981±0.05

with a 1:1 physical combination, facilitating the selection of appropriate excipients for suitability. The study of the DSC thermograms indicated a unique melting point for the extract, slightly different to 90.37°C and 331.18°C. The DSC thermograms of HPMC K100 displayed melting points at 59.30°C. The absence of a shift indicates stability between the extract and HPMC K100. Figures 3 and 8-10 illustrate the compared DSC thermograms for the extracts, individual excipients, and drug-excipient mixtures. The DSC thermograms of both extracts and physical mixes exhibited two endothermic peaks corresponding to the polymer, whereas the melting endotherm of the extract emerged due to the amorphization or diluting impact of the polymer [19,20]. Also thermal analysis results demonstrated that no chemical interaction occurred between extract and HPMC K100.

Formulation Designs

Statistical analysis of Tensile strength (Y1)

When developing new Patch formulations, it is crucial to take the tensile strength of the patches in consideration. The mixtures that improved the material's tensile strength included glycerol as a plasticizer. Table 3 displays the coded levels of the dependent variables in addition to the findings of the tensile strength of all the formulations.

From 0.567 to 0.987 Kg/cm2 was the range of the tensile strength. The tensile strength was found to be proportional to the concentration of HPMC and PVA used in the Patches. An increase in tensile strength might have been caused by a thicker dispersion, which could have resulted from a greater polymer content. Also, the tensile strength, plasticity, flexibility, and resistance to breaking of the Patches were all enhanced by the addition of glycerol, a highly effective plasticizer. It also protected the Patch from becoming too brittle. The effect of independent variables on tensile strength is presented in Figure 11 A and B. The following is the polynomial equation that represents the tensile strength (Y1).

$$Y1 = +0.5935-0.0480{*}A-0.0482{*}B-0.0147{*}C-0.0025{*}AB+0.0360{*}AC+0.0390{*}BC+0.0181{*}A^2+0.0391{*}B^2+0.0731{*}C^2 \ldots\ldots\ldots\ldots (2)$$

The formulation development process is represented by this polynomial equation, where Y1 is the tensile strength, A is the concentration of HPMC, B is the concentration of PVA, and C is the concentration of glycerol. The tensile strength was significantly affected by all of these independent factors ($p<0.05$). Additionally, the model's F value of 6.16 indicates statistical significance. According to Table 4, the quadratic model was proposed for Y1. With an R2 value of 0.8471, the Quadratic model was determined to be a good match for Y1. With a p-value of 0.0044, the Y1 model was determined to be statistically significant. The effect of

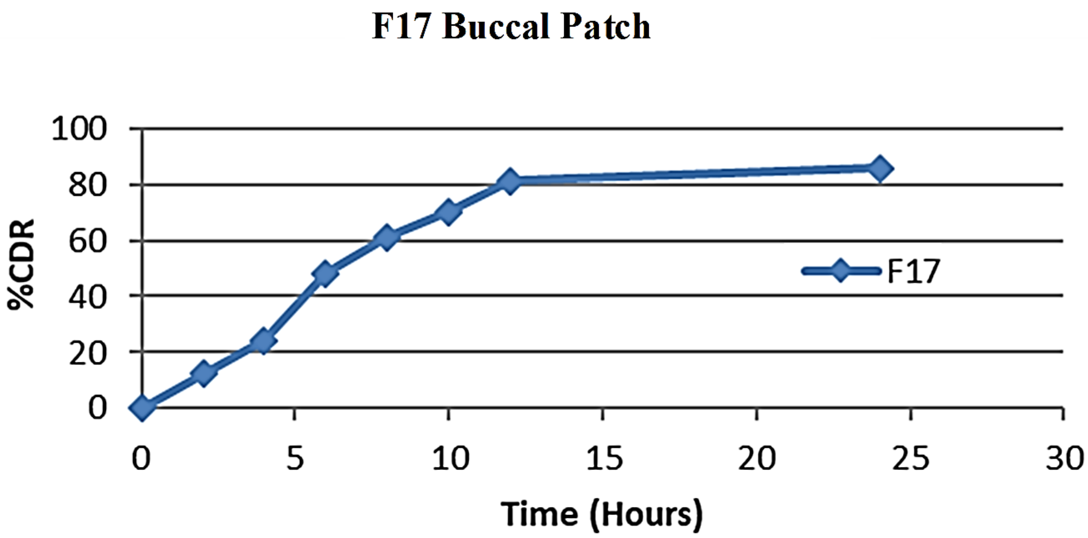

Figure 13. *In-vitro* release profile of optimized buccal patch

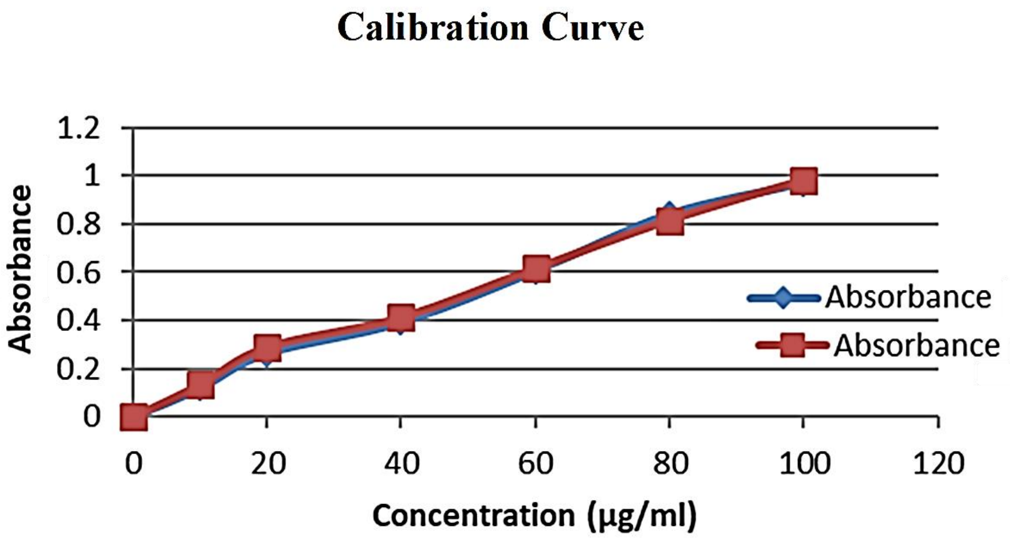

Figure 14. Standard calibration curve of both extracts in pH 6.8

Table 10. Physicochemical characterstic of Buccal Patch (stability studies)

Month	Film type	Thickness (mm)	Weight Uniformity (mg)	Folding endurance	Moisture Loss (%)	Drug content (%)	Drug release (%)
0	F17	0.291±0.06	9.87±0.12	272.1±0.21	4.1±0.07	94.25±0.77	85.74±0.21
2	F17	0.287±0.03	9.77±0.19	275.1±0.15	4.4±0.09	93.85±0.41	85.14±0.18

independent variables was also found to be statistically significant based on the *p*-value shown in Table 4.

Statistical analysis of drug release (Y2)

The drug release study was conducted in pH 6.8 phosphate buffer. At the end, the drug release was found to be in the range of 85.74% to 97.21%. It has been observed that F17 formulation with higher amount of HPMC and PVA showed excellent drug retarding property in comparison to other formulations. The effect of drug release was found to be concentration dependent. It was observed that, plasticiser in the form of glycerol at lower concentration helped to retard the drug release form the formulation Figure 12 A&B.

The polynomial equation for DR (Y2) can be presented below

$$Y2 = +91.27+0.3026^{*}A+0.8140^{*}B-0.6649^{*}C-0.3363^{*}AB-1.67^{*}AC-1.97^{*}BC \ldots\ldots\ldots\ldots (3)$$

A, B, and C are the concentrations of the independent variables employed in the construction of the formulation: %CDR, HPMC, PVA, and glycerol, respectively, in the equation mentioned above. The impact of all these independent factors on DR was statistically significant ($p<0.05$) as shown in Table 5. Additionally, the model's F value of 3.31 indicates statistical significance. For Y2, the 2FI model was recommended (Table 5). A good fit model of 2FI was shown by the correlation coefficient (R2) of 0.6046 for Y1.

Evaluation of Both Extracts-Loaded Patch

Patch Thickness

The 2 cm2 thicknesses of the patches from bathes F1 to F20 were assessed. The created patch was determined to be of consistent thickness. Table 6 displayed the results. No statistically significant difference was recorded across the formulated batches as $P > 0.05$. From this, it was concluded that the amount of patch forming polymer used increases the thickness of the patch. Consistent patch thickness is essential for optimal drug administration and patient comfirt. Fluctuations in the thickness of transdermal patches may influence the active ingredient's release kinetics and the overall performance of the system.

Uniformity of Weight of the patch

The changes in weight suggest that multiple patches taken from different areas of the baths from F1 to F20 formed with similar weight as described in Table 6. From this result, it was concluded that as the concentration of patch-forming polymer increases, the weight of the patch increases.

Folding endurance

The folding endurance results of the buccal patch are presented in Table 6. These findings suggest that the patch maintains its structural integrity within the patch pocket without breaking. A folding endurance exceeding 250 times indicates that the formulations possess desirable patch characteristics. Table 6 demonstrates an inverse relationship between the concentration of the patch-forming polymer, HPMC K100, and the number of times the patch can be folded. As the HPMC K100 concentration increases, the patch becomes more brittle, resulting in reduced folding capability.

Drug content uniformity of patch

The patch content is displayed in Table 7. While conducting the content uniformity tests, it was found that all patches broadly possessed the same concentration of the drug, confirming the reproducibility of the technique.

Moisture Loss (%)

Table 7 shows the moisture content of the patch. The moisture levels in the preparations assist in preventing the complete dissolution or brittleness of the patch.

Tensile strength of the patch

Table 7 details the strength of the patch, demonstrating that the patch displays good tensile strength which indicates that the patch would remain intact while stored in the patch pocket. From this investigation, it was established that the greater the concentration of the patch forming polymer HPMC K100, the greater the strength of the patch.

In vitro release studies

The results of *in-vitro* release study of buccal patch were performed in buffer pH 6.8 and showed that the formulation F17 containing HPMC K100 showed ideal release of the drug in 24 hours as shown in Table 8 and Figure 13.

Calibration in Phosphate Buffer pH 6.8

A standard calibration curve was generated and demonstrated linearity within the concentration range of 10 to 100µg/ml, indicating adherence to Beer-Lambert's law. The results, presented in Table 9 and Figure 14, illustrate the relationship between the concentration of the compound and its corresponding absorbance values.

Stability study

To assess the change in physicochemical parameters due to storage, a stability study was conducted. The temperature and humidity effect was examined under conditions of 40ºC±2ºC / 75%±5% RH for 2 months in an environmental stability chamber. Evaluative analyses were done after each of the 0, 1, and 2 months. As noted in Table 10, the physicochemical attributes of the optimised formulation of buccal patch indicated that there were no significant alterations on storage. However, the strength of the patches was very low and brittle. The result shows that the buccal patch formulation was stable under the specified storage conditions.

CONCLUSION

This study effectively identified and examined *Ailanthus excelsa* and *Tridax procumbens* extracts by several analytical methods. UV-Vis spectrophotometry revealed distinct absorption peaks at 254 nm and 240 nm, whilst FTIR analysis detected functional groups including carboxylic acids, ketones, amides, and aromatic carbons, signifying different chemical compositions. DSC study elucidated thermal behavior, validating phase transitions and stability under defined circumstances. Compatibility investigations of the drug and excipient utilizing FTIR and DSC demonstrated no major chemical interactions, hence assuring formulation stability. The optimization of extract-loaded buccal patches was based on tensile strength (0.567-0.987 kg/cm²) and prolonged drug release (85.74%-97.21%). The mechanical and physicochemical assessments, encompassing thickness uniformity, weight variation, folding endurance, and drug content uniformity, confirmed the appropriateness of the patches for pharmaceutical applications. In addition, studies on moisture loss confirmed their stability under diverse situations. Overall, the study effectively designed and assessed extract-loaded buccal patches exhibiting optimal mechanical strength and regulated drug release. These findings show the potential of such formulations as an efficient drug delivery strategy, illustrating their stability, efficiency, and feasibility for pharmaceutical applications. Future research should investigate in vivo assessments to validate therapeutic effectiveness and bioavailability, along with evaluating long-term stability and patient adherence for prospective clinical applications.

REFERENCES

1. Wellen, K. E.; Hotamisligil, G. S. Inflammation, Stress, and Diabetes. *J. Clin. Invest.* 2005, *115* (5), 1111–1119. https://doi.org/10.1172/JCI200525102.
2. Chauhan, A.; Chauhan, S. B. Inflammation and Cancer. In *Inflammation and Chronic Disorders: The Secret Connection*; 2023; pp 29–61. https://doi.org/10.4240/wjgs.v4.i3.62.
3. Kumar, D.; Bhat, Z. A.; Singh, P.; Shah, M. Y.; Bhujbal, S. S. Ailanthus Excelsa Roxb. Is Really a Plant of Heaven. *Int. J. Pharmacol.* 2010, *6* (5), 535–550. https://doi.org/10.3923/ijp.2010.535.550.
4. Sapkal, P. R.; Tatiya, A. U.; Firke, S. D.; Redasani, V. K.; Gurav, S. S.; Ayyanar, M.; Jamkhande, P. G.; Surana, S. J.; Mutha, R. E.; Kalaskar, M. G.

Phytochemical Profile, Antioxidant, Cytotoxic and Anti-Inflammatory Activities of Stem Bark Extract and Fractions of Ailanthus Excelsa Roxb.: In Vitro, in Vivo and in Silico Approaches. *Heliyon* 2023, *9* (5). https://doi.org/10.1016/j.heliyon.2023.e15952.

5. Andriana, Y.; Xuan, T. D.; Quy, T. N.; Minh, T. N.; Van, T. M.; Viet, T. D. Antihyperuricemia, Antioxidant, and Antibacterial Activities of Tridax Procumbens L. *Foods* 2019, *8* (1). https://doi.org/10.3390/foods8010021.
6. Devi, K.; Soni, S.; Tripathi, V.; Pandey, R.; Moharana, B. Ethanolic Extract of Tridax Procumbens Mitigates Pulmonary Inflammation via Inhibition of NF-KB/P65/ERK Mediated Signalling in an Allergic Asthma Model. *Phytomedicine* 2022, *99*. https://doi.org/10.1016/j.phymed.2022.154008.
7. Berlin Grace, V. M.; Viswanathan, S.; David Wilson, D.; Jagadish Kumar, S.; Sahana, K.; Maria Arbin, E. F.; Narayanan, J. Significant Action of Tridax Procumbens L. Leaf Extract on Reducing the TNF-α and COX-2 Gene Expressions in Induced Inflammation Site in Swiss Albino Mice. *Inflammopharmacology* 2020, *28* (4), 929–938. https://doi.org/10.1007/s10787-019-00634-0.
8. Patel, V. M.; Prajapati, B. G.; Patel, M. M. Design and Characterization of Chitosan-Containing Mucoadhesive Buccal Patches of Propranolol Hydrochloride. *Acta Pharm.* 2007, *57* (1), 61–72. https://doi.org/10.2478/v10007-007-0005-9.
9. Rohani Shirvan, A.; Hemmatinejad, N.; Bahrami, S. H.; Bashari, A. Fabrication of Multifunctional Mucoadhesive Buccal Patch for Drug Delivery Applications. *J. Biomed. Mater. Res. - Part A* 2021, *109* (12), 2640–2656. https://doi.org/10.1002/jbm.a.37257.
10. Jafar, M.; Ali, S. Development and Evaluation of Meloxicam Solid Dispersion Loaded Buccal Patches. *J. Appl. Pharm. Sci.* 2011, *1* (3), 77–82.
11. Hao, J.; Heng, P. W. S. Buccal Delivery Systems. *Drug Dev. Ind. Pharm.* 2003, *29* (8), 821–832. https://doi.org/10.1081/DDC-120024178.
12. Pelin, I. M.; Suflet, D. M. Mucoadhesive Buccal Drug Delivery Systems Containing Polysaccharides. *Cellul. Chem. Technol.* 2020, *54* (9–10), 889–902. https://doi.org/10.35812/CELLULOSECHEMTECHNOL.2020.54.86.
13. Palem, C. R.; Gannu, R.; Doodipala, N.; Yamsani, V. V.; Yamsani, M. R. Transmucosal Delivery of Domperidone from Bilayered Buccal Patches: In Vitro, Ex Vivo and in Vivo Characterization. *Arch. Pharm. Res.* 2011, *34* (10), 1701–1710. https://doi.org/10.1007/s12272-011-1014-2.
14. Lee, R. Statistical Design of Experiments for Screening and Optimization. *Chemie-Ingenieur-Technik* 2019, *91* (3), 191–200. https://doi.org/10.1002/cite.201800100.
15. Riter, L. S.; Vitek, O.; Gooding, K. M.; Hodge, B. D.; Julian, R. K. Statistical Design of Experiments as a Tool in Mass Spectrometry. *J. Mass Spectrom.* 2005, *40* (5), 565–579. https://doi.org/10.1002/jms.871.
16. Popovici, V.; Matei, E.; Cozaru, G. C.; Bucur, L.; Gîrd, C. E.; Schröder, V.; Ozon, E. A.; Mitu, M. A.; Musuc, A. M.; Petrescu, S.; Atkinson, I.; Rusu, A.; Mitran, R. A.; Anastasescu, M.; Caraiane, A.; Lupuliasa, D.; Aschie, M.; Dumitru, E.; Badea, V. Design, Characterization, and Anticancer and Antimicrobial Activities of Mucoadhesive Oral Patches Loaded with Usnea Barbata (L.) F. H. Wigg Ethanol Extract F-UBE-HPMC. *Antioxidants* 2022, *11* (9). https://doi.org/10.3390/antiox11091801.
17. UV-VIS Spectroscopy and Its Applications. *Choice Rev. Online* 1993, *30* (11). https://doi.org/10.5860/choice.30-6183.
18. Ahmad, A.; Ayub, H. Fourier Transform Infrared Spectroscopy (FTIR) Technique for Food Analysis and Authentication. In *Nondestructive Quality Assessment Techniques for Fresh Fruits and Vegetables*; 2022; pp 103–142. https://doi.org/10.1007/978-981-19-5422-1_6.
19. Schick, C. Differential Scanning Calorimetry (DSC) of Semicrystalline Polymers. *Anal. Bioanal. Chem.* 2009, *395* (6), 1589–1611. https://doi.org/10.1007/s00216-009-3169-y.
20. Menczel, J. D.; Andre, R.; Kohl, W. S.; Krongauz, V. V.; Lőrinczy, D.; Reading, M.; Grebowicz, J. Fundamentals of DSC. In *Handbook of Differential Scanning Calorimetry: Techniques, Instrumentation, Inorganic, Organic and Pharmaceutical Substances*; 2023; pp 1–189. https://doi.org/10.1016/B978-0-12-811347-9.00005-9.